Mechanical, Thermal, and Transport Properties of Nitrile Rubber–Nanocalcium Carbonate Composites

Meera Balachandran, S. S. Bhagawan

Department of Chemical Engineering and Materials Science, Amrita Vishwa Vidyapeetham, Coimbatore 641105, India

Received 8 April 2011; accepted 23 September 2011
DOI 10.1002/app.36328
Published online in Wiley Online Library (wileyonlinelibrary.com).

ABSTRACT: The article describes the properties of acrylonitrile butadiene copolymer (NBR)–nanocalcium carbonate (NCC) nanocomposites prepared by a two-step method. The amount of NCC was varied from 2 phr to 10 phr. Cure characteristics, mechanical properties, dynamic mechanical properties, thermal behavior, and transport properties of NBR–NCC composites were evaluated. For preparing NBR nanocomposites, a master batch of NBR and NCC was initially made using internal mixer. Neat NBR and the NBR–NCC masterbatch was compounded with other compounding ingredients on a two roll mill. NCC activated cure reaction upto 5 phr. The tensile strength increased with the nanofiller content, whereas NBR–NCC containing 7.5 phr exhibited the highest modulus. The storage modulus (E') increased up to 5 phr NCC loading; the reinforcing effect of NCC was seen in the increase of modulus which was more significant at temperatures above T_g. The effect of nanofiller content and temperature on transport properties was evaluated. The solvent uptake decreased with NCC content. The mechanism of diffusion of solvent through the nanocomposites was found to be Fickian. Transport parameters like diffusion, sorption, and permeation constants were determined and found to decrease with nanofiller content, the minimum value being at 7.5 phr. Thermodynamic constants such as enthalpy and activation energy were also evaluated. The dependence of various properties on NCC was supported by morphological analysis using transmission electron microscopy. © 2012 Wiley Periodicals, Inc. J Appl Polym Sci 000: 000–000, 2012

Key words: nanocomposite; mechanical properties; swelling; thermal properties; rubber

INTRODUCTION

Both natural rubber and synthetic rubbers find a wide range of industrial applications such as automotive parts, construction materials and machine components. Usually, they are reinforced with particulate fillers like carbon black, silica etc. to improve various properties. The improvements in properties by using particulate fillers are achieved by the physical interaction between the filler and the elastomer matrix. In the last two decades, usage of nanofiller has attracted ample attention due to large improvement in mechanical, thermal, and barrier properties. Significantly, these improvements are achieved at very low filler concentrations compared with conventional micro fillers. Nanoclay, nanosilica, nanocalcium carbonate (NCC), nanoalumina etc. are some of the popularly studied nanofillers. Among the nanofillers, nanoclay is the most widely studied. Several studies have reported on the effect of nanoclay concentration, type of organo modifier, and effect of preparation methods on the properties of polymer–nanoclay composites.[1–5] and references therein The improvement in properties of nanoclay reinforced composites is attributed to its high aspect ratio and large surface area.

The mechanical properties of particulate-filled polymer micro and nanocomposites are affected by particle size, particle content and particle/matrix interfacial adhesion.[6] Spherical nanofillers have low aspect ratio and large surface area.[7] NCC is a particulate nanofiller that has advantages in terms of cost and commercial availability compared with nanoclay or nanofibers. There are several studies on the effect of nanometric calcium carbonate on properties of thermoplastic polymers, especially polypropylene (PP). Several studies show that that incorporation of nano-$CaCO_3$ particles remarkably improved the thermal stability, mechanical properties, dynamic rheological properties, and crystallization rate in PP composites.[8–11] Addition of NCC and elastomer in PP develop a synergistic toughening effect on PP while retaining the strength and modulus of virgin PP.[12] The reinforcing effect of NCC in polyethylenes and polyvinyl chloride has been demonstrated in various studies.[13–16] In recent years, similar studies have been done on other thermoplastics and thermosets filled with NCC.[17,18]

Although the volume of literature on NCC filled thermoplastics and thermosets is relatively large, reported studies on nanometric calcium carbonate

Correspondence to: S. S. Bhagawan (ss_bhagawan@cb.amrita.edu).

filled elastomers are scarce. It has been reported that nanoCaCO3 increases the mechanical properties in rubbers. NCC was found to improve the tensile properties and thermooxidative aging resistance properties of natural rubber composites.[19,20] In butadiene rubber NCC increased tensile strength, elongation, mechanical interfacial properties, toughness, hardness, and thermal stability while reducing the flammability.[21] Mishra and Shimpi have reported that reduction in nanosize of $CaCO_3$ brings about drastic improvement in mechanical properties, swelling index, flame retardancy, and abrasion resistance of styrene butadiene rubber compared with microsize $CaCO_3$.[22–24] Studies on ethylene propylene diene monomer (EPDM) matrix showed that the incorporation of methacrylic acid improved the interfacial interaction between nano-$CaCO_3$ particles and EPDM matrix, leading to enhancement in the mechanical properties of filled vulcanizated.[25]

Acrylonitrile–butadiene copolymer, commonly known as nitrile rubber (NBR), is a special purpose elastomer used in applications that require oil resistance. Earlier, we found that incorporation of nanoclay into the NBR matrix effectively reinforced the rubber matrix. While there are several studies that have reported tremendous property improvement in NBR–nanoclay composites,[26–32] there are very few studies on nanometric $CaCO_3$ filled nitrile rubber (NBR) composites. Przepiórkowska et al. used nanosized chalk to obtain XNBR and NBR rubber vulcanizates with very good mechanical properties, good resistance to thermal aging, and increased water absorption capability.[33] Yueyi reported that the mechanical properties of NBR vulcanizates had been improved by nano-$CaCO_3$ modified with borate coupling agent.[34] As discussed earlier, nano-$CaCO_3$ filler gave remarkable improvements in rubbers like natural rubber, SBR, EPDM, and butadiene rubber. The use of NCC in NBR has not been studied extensively earlier, in this article, we have investigated the effect of NCC on mechanical, thermal, and transport properties of nitrile rubber and the properties have been compared with those of NBR–$CaCO_3$ vulcanizates.

This article describes the preparation of NCC–NBR composites by a two-step method. The cure characteristics, mechanical and dynamic mechanical properties, and transport behavior of NBR nanocomposites reinforced with different levels of NCC were studied. The morphological studies on the NBR nanocomposites were carried out using transmission electron microscopy (TEM).

EXPERIMENTAL

Materials

Nitrile rubber (NBR) with 33% acrylonitrile content and having Mooney viscosity of ML (1 + 4) at 100°C = 47.0 was procured from Apar Industries, Mumbai, India. NCC of average particle size <40 nm (specific gravity 2.52, oil absorption 33–36 mL/100 g) was provided by KPS Consultants & Impex, New Delhi, India. Other compounding ingredients were obtained from standard suppliers in India. The formulation used for the study included NBR (100 phr), sulfur (1.5 phr), zinc oxide (5 phr), stearic acid (1 phr), NCC (varied), dioctyl phthalate (DOP, varied maintaining NCC : DOP ratio at 4 : 1), dibenzothiazole disulfide (MBTS, 1.25 phr), and tetramethyl thiuram disulfide (TMTD, 0.25 phr). Precipitated calcium carbonate of particle size 0.7 micron was used in the formulation for comparison.

Preparation of NBR nanocomposites

NBR nanocomposites were prepared by a two-step method. In the first step, a masterbatch of NCC and NBR in the ratio three parts rubber : 1 part nanofiller by weight was made using Fissions Haake Rheocord 90. To prepare the masterbatch, NBR was first masticated at 60 rpm till the torque stabilized, after which NCC was added and mixing continued for 10 min. The NBR–NCC masterbatch was then compounded with neat NBR and other compounding ingredients in a two roll mill with friction ratio 1.25. Nanocomposites with varying contents of NCC were prepared. The rubber formulations were evaluated for cure characteristics on an oscillating disc rheometer (Tech-Pro Rheotech ODR-ASTM D-2084). The NBR–NCC composites were compression molded at 150°C and 200 kg/cm^2 for the optimum cure time in a hydraulic press to make approximately 2-mm thick rubber sheets. The samples were designated NBRNCCX, where X is the amount of NCC (0, 2, 5, 7.5, and 10 phr). Thus NBRNCC5 indicates NBR–NCC composite having a filler loading of 5 phr. Composites with precipitated calcium carbonate were also prepared with the same formulation for comparison.

Characterization

The morphology of the nanocomposites were examined by TEM images taken with JEOL 2010 electron microscope with accelerator voltage of 200 kV. The nanocomposite samples for TEM analysis were prepared by ultra cryomicrotomy at −80°C using Leica Ultracut UCT. Freshly sharpened glass knives with cutting edge of 45° were used to get cryosections of 100-nm thickness.

To evaluate the stress–strain properties (tensile strength, modulus, and elongation at break) dumbbell specimens were punched out from the molded sheets and tested as per ASTM D412 method on a Universal Testing Machine at a crosshead speed 500 mm/min. For all mechanical properties, the average of five experimental values is reported.

TABLE I
Cure Characteristics of NBR–NCC Composites at 150°C

Name	NCC content (phr)	Scorch time (min)	Cure time (min)	τ_{min} (Nm)	τ_{max} (Nm)	$\Delta\tau$ (Nm)	Cure rate index (CRI; min^{-1})
NBRNCC0	0	3.5	10.2	0.43	2.78	2.35	14.84
NBRNCC2	2	3.5	8.0	0.40	3.02	2.62	21.93
NBRNCC5	5	3.5	7.1	0.31	2.79	2.48	28.17
NBRNCC7.5	7.5	3.3	9.1	0.36	2.86	2.50	17.30
NBRNCC10	10	3.3	8.4	0.38	2.78	2.40	19.61

Dynamic mechanical analysis was done using DMA Q800. Rectangular specimens having dimensions 35 × 12 × 2 mm were used. The dynamic moduli and mechanical damping (tan δ) were evaluated. The dynamic analysis was done in dual cantilever mode with temperature scan from −70 to +70°C using heating rate of 2°C/min at 1 Hz and 10 Hz.

The thermal stability of the samples from 35 to 500°C was investigated using NETZSCH STA 409 CD TGA-DTA simultaneous analyzer at a heating rate of 10°C/min in nitrogen atmosphere.

Transport properties were studied using rectangular samples of size 20 × 20 mm cut from the NBR–NCC composites. The edges of the samples are slightly curved to obtain uniform absorption. The thickness and initial weight of samples were measured. The samples were completely immersed in toluene in glass diffusion bottles kept at uniform temperature. The samples were removed from the solvent at specific time intervals, excess solvent at the surface removed using filter paper and weighed. The samples were returned to the solvent in the diffusion bottle immediately. The process was continued until constant weight, indicating that equilibrium swelling was reached. The mole percent uptake (Q_t) of solvent at time, t, of immersion was determined using the formula

$$Q_t = \frac{(M_t - M_o)/M_W}{M_o} \times 100 \quad (1)$$

where M_t is the mass of sample after time t of immersion, M_o the initial mass of the sample and M_w is the molecular weight of the solvent. The sorption isotherms were analyzed using plots of mole percentage uptake of solvent versus square root of time. The diffusion and permeability coefficients were then calculated. The experiments were conducted at 30, 50, and 70°C. The values reported here are the averages of three experiments.

RESULTS AND DISCUSSION

Cure characteristics

The curing behavior of the composites was analyzed at 150°C on a TechPro Rheotech oscillating disc cure meter. The cure characteristics of NBR nanocomposites are summarized in Table I. It is observed that addition of NCC had no effect on the scorch time (t_{s2}) of the nanocomposites upto 5 phr. However, at higher NCC content, there was a slight reduction in scorch time. The cure time (t_{90}) of the compounds showed a decrease on incorporation of NCC upto 5 phr and thereafter increased at higher NCC content. It may be inferred that the NCC activated the cure reaction upto 5 phr. At higher nanofiller content, the activation may be lesser due to agglomeration of the particles as evident from morphological studies. Cure rate index (CRI), a direct measure of the fast curing nature of the rubber compounds, was calculated using the following relation[35]:

$$\mathrm{CRI} = 100/[t_{90} - t_{s2}] \quad (2)$$

For the NBR nanocomposites, CRI increased with addition of NCC and it supported the activation of cure reaction up to 5 phr. On further increase in the filler content, cure time increased while CRI decreased, but was higher than unfilled NBR. At higher loading, a deactivation of the cure process was observed due to the increase of t_{90} values, resulting in a poor interfacial interaction between rubber and NCC, which confirmed the formation of aggregates of NCC in the filled compounds.[35]

From the study on the effect of NCC content on rheometric torque of NBR nanocomposites, it is observed that the minimum torque (τ_{min}), an indirect measure of viscosity of the compound, decreased as NCC loading increased to 5 phr and thereafter showed an increase. However, no such trend was observed for the maximum torque (τ_{max}) of NCC filled NBR. The difference between maximum and minimum torques ($\Delta\tau$) was found to increase for the nanocomposites upto 5 phr. This difference is an indication of the extent of crosslinking.[36,37] This may be due to the interaction between the NCC and the rubber matrix, the interaction being enhanced by the larger interfacial area between the nanofiller and the matrix. However, at NCC content greater than 5 phr, $\Delta\tau$ decreased. This may be due to the reduction in interaction between the nanofiller and NBR due to agglomeration of NCC.

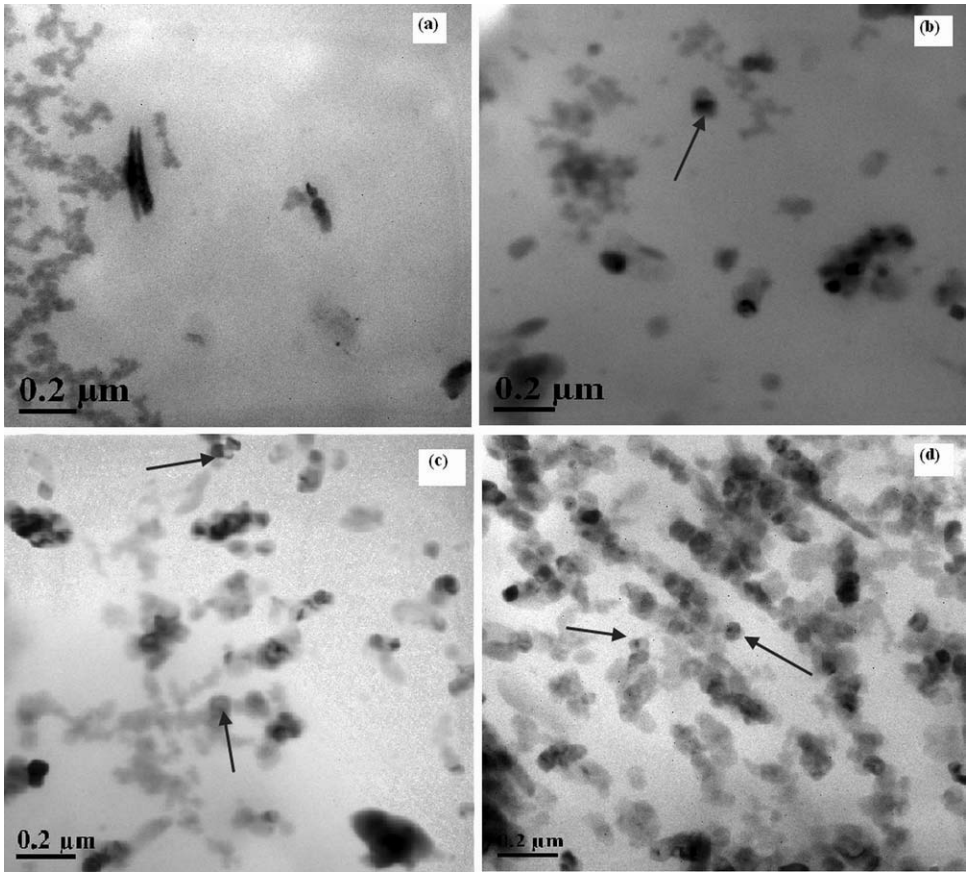

Figure 1 TEM micrographs of NBR–NCC composites (a) 0 phr (b) 2 phr, (c) 5 phr, and (d) 10 phr.

Morphology

TEM was used to study the nanostructure of NBR–NCC composites. The TEM micrographs of NBR nanocomposites containing 0, 2, 5, and 10 phr are shown in Figure 1(a–d), respectively. The cubical NCC particles are indicated by the arrow in the figure. It was observed that NCC was finely and uniformly dispersed in composites containing 2 and 5 phr. However, as the filler content was increased to 10 phr, the NCC was found to form aggregates. From the TEM micrographs, it may be concluded that at higher NCC contents, strong particle–particle interaction caused the formation of agglomerates. In EPDM rubbers, the formation of agglomerates has been attributed to the high surface energy of NCC.[25]

Mechanical properties

The stress–strain curves of the NBR–NCC composites are shown in Figure 2. It is seen that the stress continuously increased with deformation of NBR; the stress–strain behavior is typical of synthetic elastomers. Compared with neat NBR, incorporation of NCC increased the stress in the nanocomposites for the same strain level. The mechanical properties of NBR nanocomposites with different NCC contents are given in Table II. It is observed that the tensile strength increased with the NCC content. The increase in the tensile strength was 24% and 42% for 5 and 10 phr of NCC, respectively. This was equivalent to the increase in tensile strength from 10 phr and 20 phr respectively of commercial precipitated $CaCO_3$. To get an equivalent increase in tensile strength using commercial precipitated $CaCO_3$, the filler content should be two times that of NCC. The modulus at 100% elongation increased up to 7.5 phr

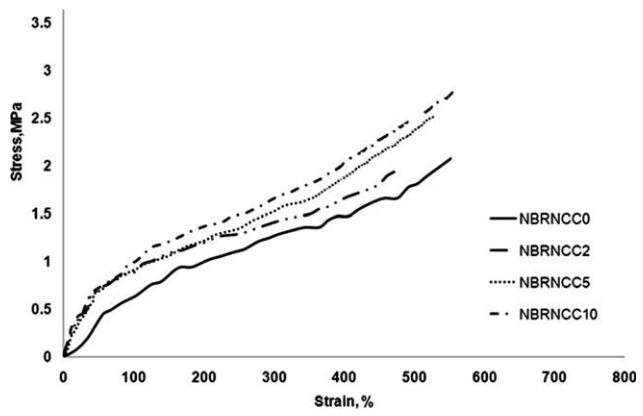

Figure 2 Stress–strain characteristics of NBR–NCC composites.

TABLE II
Mechanical Properties of NBR–NCC Composites

Name	NCC content (phr)	Precipitated $CaCO_3$ content (phr)	Tensile strength (MPa)	Elongation at break (%)	M100 (MPa)	M300 (MPa)	M_{100f}/M_{100u}
NBRNCC0	0	0	2.19	558	0.54	0.97	1.00
NBRNCC2	2	0	2.20	458	0.87	1.08	1.61
NBRNCC5	5	0	2.62	519	1.01	1.30	1.87
NBRNCC7.5	7.5	0	2.72	436	1.16	1.64	2.15
NBRNCC10	10	0	3.11	503	0.93	1.27	1.72
NBRCC10	0	10	2.81	521	0.89	1.16	1.65
NBRCC20	0	20	3.09	582	1.03	1.29	1.91
NBRCC30	0	30	2.89	556	0.96	1.28	1.77
NBRCC40	0	40	2.78	562	0.95	1.19	1.76

and then decreased. It may be noted that by adding 5 phr of NCC, the modulus obtained is comparable with that obtained by adding 20 phr of precipitated $CaCO_3$. The reinforcing effect of the NCC was evident from the increase in the ratio of modulus of filled compounds (M_{100f}) to that of unfilled NBR (M_{100u}). The improvement in mechanical properties of the nanocomposites, which was greater than that produced by equivalent quantity of precipitated calcium carbonate, was due to the smaller dimension of the NCC, resulting in larger surface area of the filler and better interfacial bonding with the rubber matrix. This, along with good dispersion and homogeneity in bonding, improved the mechanical properties of the nanocomposites.[23,37] In natural rubber, the reinforcing ability of the NCC has been attributed to the smaller particle size, greater surface area and consequently increased contact area between the filler and rubber particles. This inhibited the movement of polymer chains while increasing the ability to inhibit microcrack expansion.[38] But as the amount of the reinforcing filler exceeds a critical value, the contact between the rubber and filler gets saturated. Further increase in filler content causes agglomeration and the distance between rubber particles and agglomerates tends to increase, thus making the filler and rubber behave as different phases resulting in poorer reinforcing effect.[38] Similar improvement in tensile properties for NCC-based composites of natural rubber,[39] butadiene rubber,[21] SBR[23] and NR, and NR/NBR blends[20] was reported in the literature.

Dynamic mechanical behavior

The dynamic elastic (storage) modulus E' data for neat NBR and NBR–NCC composites are plotted as a function of temperature in Figure 3. Above T_g, at all loadings of NCC, the nanocomposites showed clear enhancement in storage modulus. The enhancement in E' further corroborated the effect of higher interaction between the NCC and the rubber matrix, discussed earlier in the text. However, below T_g, the difference in the values of E' was less significant. The effectiveness of the filler on the moduli of the composites may be represented by the coefficient C calculated using[40]

$$C = (E'_G/E'_R)_{\text{composite}}/(E'_G/E'_R)_{\text{resin}} \quad (3)$$

where E'_G and E'_R are the storage modulus values in the glassy and rubbery region, respectively. Here, resin represents the unfilled rubber. Higher the value of the coefficient C, lower the effectiveness of the filler. The measured values of E' at $-50°C$ and $+50°C$ were used as E'_G and E'_R, respectively. It was noted from the values of C, given in Table III, that the effectiveness of the filler was optimum at 7.5 phr. At this concentration, the stress transfer between the matrix and the filler was maximum. The effectiveness of NCC is comparable that of precipitated $CaCO_3$ having double the concentration.

The effect of NCC content on loss factor (tan δ) as a function of temperature at a frequency of 1 Hz is shown in Figure 4. It is observed that the effect of NCC content on the peak value of tan δ and T_g values of the NBR–NCC composites is marginal. The area under the peak in tan δ versus temperature curve is a measure of energy dissipated. As

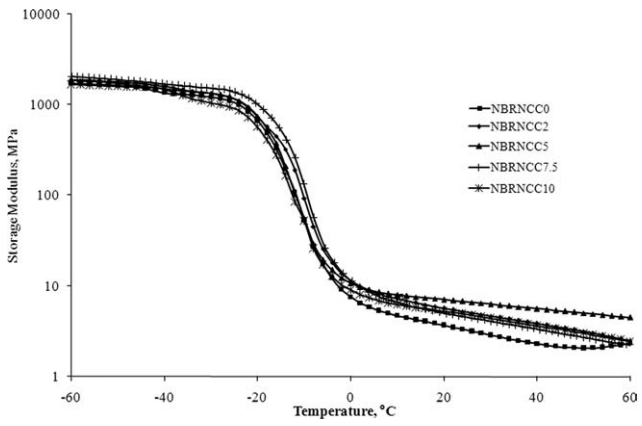

Figure 3 Storage modulus (E') as a function of temperature for NBR–NCC composites at 1 Hz.

TABLE III
Dynamic Mechanical Analysis of NBR–NCC Composites at 1 Hz

Sample	Tan δ_{max}	E''_{max} (MPa)	T_g from tan δ (°C)	T_g from E'' (°C)	C
NBRNCC0	1.30	221	−8.0	−14.0	1.00
NBRNCC2	1.35	166	−9.9	−14.0	0.72
NBRNCC5	1.26	222	−9.2	−16.0	0.43
NBRNCC7.5	1.44	248	−8.0	−13.8	0.40
NBRNCC10	1.26	177	−12.0	−16.0	0.67
NBRCC10	1.24	192	−12.8	−18.0	0.43

observed from the figure, there is marginal narrowing of peaks and marginal reduction of damping properties. The effect of NCC content on values of tan δ_{max}, E''_{max}, and the T_g values obtained for all the samples at 1 Hz is tabulated in Table III. The maximum value of tan δ is greater than that of unfilled NBR at 2 and 7.5 phr, indicating better damping properties at these values. But at other NCC contents, it is lower than neat NBR. The maximum value of loss modulus was observed to be at 7.5 phr of NCC. The T_g generally decreased on addition of NCC, except for 7.5 phr NCC content. The dynamic mechanical properties of NBR–NCC composite at 7.5 phr may be different due to the increased NCC–NCC interaction and interphase properties at this critical filler content.

Thermal behavior

The thermal stabilities of NBR/nano-$CaCO_3$ composites were studied by means of TGA in nitrogen atmosphere. The thermal stability factors, viz. initial decomposing temperature (IDT), temperature at the maximum rate of weight loss (T_{max}), and the char content at 500°C were calculated from the TGA thermograms and are listed in Table IV. The thermal stability of the composites was enhanced on addition of

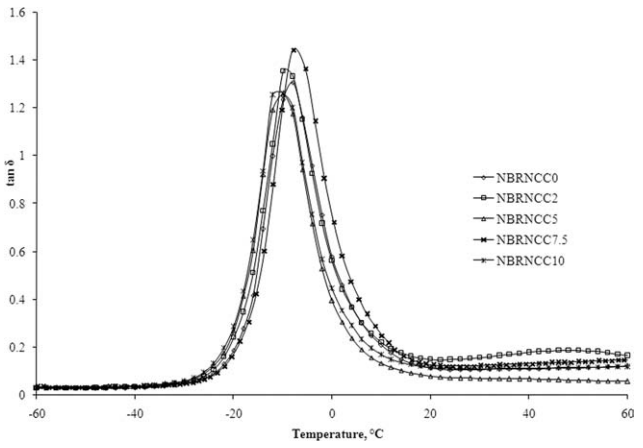

Figure 4 Effect of NCC content on tan δ of NBR–NCC composites at 1 Hz.

TABLE IV
Thermal Stability Factors of NBR–NCC Composites Obtained from TGA

Name	NCC content (phr)	IDT (°C)	T_{max} (°C)	Char (%)
NBRNCC0	0	401	450	23.0
NBRNCC2	2	407	447	25.5
NBRNCC7.5	7.5	410	447	29.1
NBRNCC10	10	412	446	32.8

NCC. In neat rubber, IDT was around 400 C. On addition of NCC, the IDT increased by 6–11°C depending on the content of the filler. The thermograms for the NBR nanocomposites are given in Figure 5. This increase in the IDT was also visible in the shoulder region of the derivative thermograms shown in Figure 6. Another notable feature from the derivative thermogram was that the maximum rate of decomposition of the nanocomposites decreased significantly on addition of NCC. This is clearly evident in the reduction in peak height of the derivative thermogram with increasing NCC content. However, NCC content had no significant effect on the temperature at which maximum rate of decomposition occurs. Jin and Park[21] postulated that the increased area of contact of the nanometric $CaCO_3$ with the rubber matrix increases the absorption of heat energy during decomposition, resulting in higher IDT and lower decomposition rate for the nanocomposites. The char content of the nanocomposites at 500°C increased with NCC content.

Transport characteristics

The effects of NCC concentration on the diffusion, sorption, and permeation of toluene through NBR

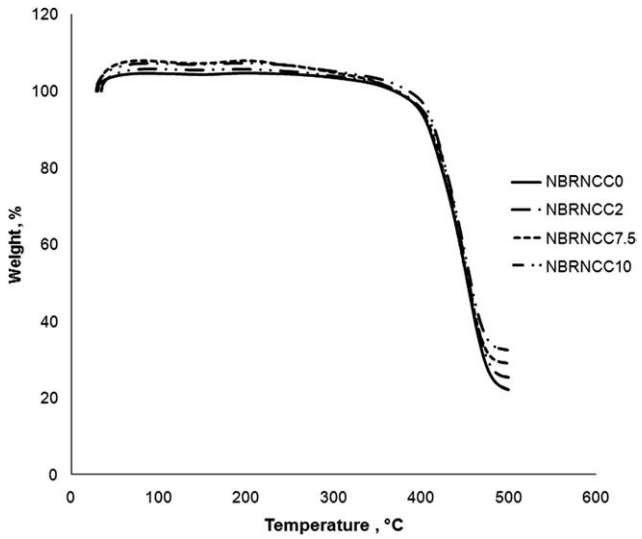

Figure 5 Thermograms for NBR–NCC composites.

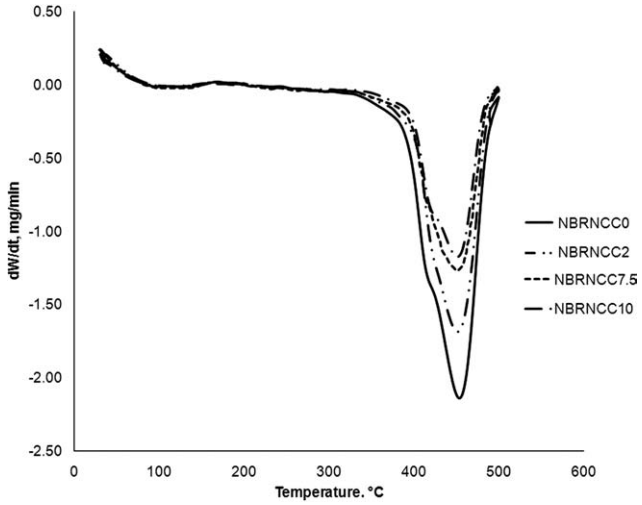

Figure 6 Derivative thermograms for NBR–NCC composites.

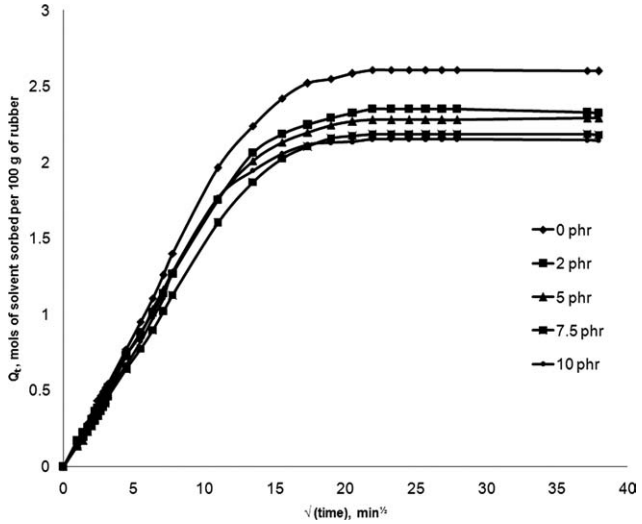

Figure 7 Sorption isotherms for NBR–NCC composites at 30°C.

nanocomposites were studied. The transport behavior through composites depends on filler type, matrix, temperature, reaction between solvent and the matrix etc. Hence, the study of the transport process through composites can be used as an effective tool to understand the interfacial interaction and morphology of the system. The swelling behavior of NBR–NCC composites was assessed by calculating swelling coefficient (β) using the equation[41]

$$\beta = \frac{(M_\infty - M_o)}{M_o} \times \rho_s^{-1} \tag{4}$$

where M_o and M_∞ are the mass of the sample before swelling and at equilibrium swelling, respectively, and ρ_s is the density of the solvent. Table V shows that the swelling coefficient decreased with increase in NCC content. The sorption curves were plotted as Q_t (moles of solvent sorbed per 100 g of rubber) against $\sqrt{}$(time). As evident in Figure 7, the curves showed two distinct regions—an initial steeper region with high sorption rate due to large concentration gradient and a second region exhibiting reduced sorption rate that ultimately reached equilibrium sorption. The sorption rate and equilibrium solvent uptake of NBR nanocomposites reduced with increasing NCC content. However, at 10 phr the sorption rate was reduced. Beyond 7.5 phr, there was no appreciable change in equilibrium solvent uptake. This was due to the formation of agglomerates of NCC which was evident from the TEM micrographs.

TABLE V
Swelling Coefficient of NBR–NCC Composites

Sample	Swelling coefficient (β) (cm^3/g)
NBRNCC0	2.77
NBRNCC2	2.49
NBRNCC5	2.43
NBRNCC7.5	2.32
NBRNCC10	2.28

The diffusivity D of the nanocomposites was calculated using eq. (5)[42–45]

$$D = \pi(h\theta/4Q_\infty)^2 \tag{5}$$

where h is the thickness of the sample, θ is the slope of the sorption curves before attaining 50% equilibrium (the initial linear portion of the curve), and Q_∞ is the equilibrium solvent uptake.

The sorption coefficient was calculated using the eq. (6)[42–45]

$$S = M_s/M_o \tag{6}$$

where M_s is the mass of solvent taken up at equilibrium swelling and M_o is the mass of the sample.

The net diffusion through polymer depends on the difference in the amount of penetrant molecules between the two surfaces. Hence, the permeability can be expressed as[42–45]

$$P = D \times S \tag{7}$$

where D is the diffusivity and S is the solubility, taken as mass of solvent sorbed per unit mass of the sample.

The diffusion, sorption, and permeability coefficients of NBR–NCC composites at 30, 50, and 75°C are given in Table VI. The diffusion and permeation coefficients of the nanofilled composites were considerably lower than the unfilled NBR. The diffusion of the penetrant solvent depended on the concentration of free space available in the matrix to

TABLE VI
Transport Coefficients and Thermodynamic Parameters of NBR–NCC Composites

Sample	Diffusion coefficient ($D \times 10^7$) m^2/s			Sorption coefficient (S) (g/g)			Permeability coefficient ($P \times 10^7$) (m^2/s)			E_D (kJ/mol)	E_P (kJ/mol)	ΔH_s (kJ/mol)
	30°C	50°C	75°C	30°C	50°C	75°C	30°C	50°C	75°C			
NBRNCC0	6.58	8.11	8.46	2.39	2.30	2.16	15.7	18.6	18.3	4.86	2.88	−1.98
NBRNCC2	6.19	8.00	8.43	2.14	2.22	1.89	13.2	17.7	15.9	5.95	3.51	−2.44
NBRNCC5	5.92	7.96	8.32	2.11	2.01	1.79	12.5	16.0	14.9	6.56	3.41	−3.15
NBRNCC7.5	5.53	7.04	8.03	2.01	1.95	1.84	11.1	13.7	14.8	7.23	5.55	−1.68
NBRNCC10	5.93	7.78	7.78	1.97	1.87	1.83	11.7	14.5	14.2	6.21	3.66	−2.55

accommodate the penetrant molecule.[43] The addition of NCC reduced the availability of these free spaces and also restricted segmental mobility of the rubber matrix. However, at 10 phr, there was an increase in diffusion and permeation coefficients. This increase was due to the aggregation of the nanofiller. Similar trends were observed for sorption studies conducted at 50°C and 75°C. As the temperature increased, the coefficient of diffusion also increased for all the samples. As temperature increased, the thermal energy increased and consequently molecular vibration of solvent molecules, the free void volume in the polymer matrix and flexibility of the polymer chains increased.[46] As a result, the diffusion coefficients of the NBR composites increased with temperature. Maiti et al. had reported similar reduction in transport coefficients for fluoroelastomer–clay nanocomposites.[45]

The energy required for the diffusion or permeation of solvent molecule was computed using Arrhenius equation[35]

$$X = X_0 e^{-E_x/RT} \tag{8}$$

where X is D or P, X_o is a constant representing either D_o or P_o (diffusion and permeation coefficients extrapolated to zero permeant concentration), R is the gas constant, T is the temperature in Kelvin and E_x is the activation energy. The activation energy of diffusion of toluene through NBR nanocomposites was found to be higher than that of unfilled elastomer. The nanofillers have higher specific surface area resulting in greater rubber–filler interaction and enhanced reinforcement. As the nanofiller content increased, the activation energy needed for diffusion also increased. The activation energy for permeation (E_P), also evaluated using the Arrhenius equation, showed similar trend as E_D. The enthalpy of sorption ΔH_s was determined by van Hoff equation.[47]

$$E_P = \Delta H_s + E_D \tag{9}$$

It is observed that the sorption is an exothermic process. The value of ΔH_s increased with increasing nanofiller content.

To evaluate the mechanism of sorption, the solvent uptake data of the nanocomposites were fitted to the equation[43,44]

$$\log\,(Q_t/Q_\infty) = \log\, k + n\, \log\, t \tag{10}$$

where "Q_t" is the mol% uptake at time "t," Q_∞ is the mol % uptake at equilibrium and "k" is a constant characteristic of the interaction between the sample and solvent. The values of n and k determined by linear regression analysis are shown in Table VII. Generally, the diffusion behavior of polymeric composites can be classified according to the relative mobility of the penetrant and of the polymer segments into (i) Case I or Fickian diffusion, (ii) Case II diffusion, and (iii) non-Fickian or anomalous diffusion. For a Fickian mode of diffusion, the value of n is equal to 0.5 and the predominant driving force for diffusion is the concentration gradient. The rate of diffusion is much less than the rate of

TABLE VII
Parameters for Diffusion Mechanism of Toluene through NBR–NCC Composites

Sample	30°C		50°C		75°C	
	n	k (g/gmin^2)	n	k (g/gmin^2)	n	k (g/gmin^2)
NBRNCC0	0.48	0.076	0.50	0.068	0.51	0.071
NBRNCC2	0.47	0.082	0.49	0.071	0.51	0.073
NBRNCC5	0.49	0.073	0.49	0.067	0.50	0.067
NBRNCC7.5	0.48	0.076	0.50	0.065	0.51	0.069
NBRNCC10	0.48	0.082	0.48	0.073	0.53	0.069

relaxation of polymer chains. In Case II diffusion, n is equal to 1 and the rate of diffusion is much higher than the relaxation process. When the value falls between 0.5 and 1, the diffusion is anomalous and the rate of diffusion becomes comparable with the rate of relaxation of polymer chains.[48] In the case of NBR–NCC nanocomposites, the value of "n" at room temperature (30°C) is close to 0.5 and the diffusion is fickian type, controlled by concentration dependent diffusion coefficient. In rubbery polymers, well above their glass transition temperatures, the polymer chains adjust quickly to the presence of penetrant molecules and hence they do not exhibit anomalous behavior. It is observed that as the temperature increased, the value of n increased for NBR–NCC composites, implying that the diffusion tended to be of anomalous type. The constant k decreased with increasing temperature.

CONCLUSION

NBR–NCC composites were prepared from a masterbatch of NBR and NCC in an internal mixer followed by mixing on a two-roll mill. The cure time of the compounds showed a decrease on incorporation of NCC upto 5 phr and thereafter increased at higher NCC content. NCC activated the cure reaction upto 5 phr. The tensile strength and modulus increased with NCC content. The dispersion of NCC in NBR matrix was analyzed from transmission electron micrographs. The mechanical properties of NBR–NCC nanocomposites were found to be superior to those of NBR-$CaCO_3$ microcomposites. Investigation of dynamic mechanical properties showed that addition of NCC increased and lowered the tan δ peak value, without altering the T_g of the nanocomposite. Addition of NCC to NBR resulted in enhanced thermal stability. The sorption of toluene through the nanocomposite decreased with increasing NCC content. The diffusion, sorption, and permeation coefficients for diffusion of toluene through NBR–NCC composites were found to decrease with nanofiller content. The values of the transport coefficients were slightly higher at 10 phr NCC content than at 7.5 phr because of aggregation of the nanofiller. Activation energy for diffusion and permeation for the nanocomposites were higher than that of neat NBR. Diffusion of toluene through NBR–NCC composites was found to exhibit Fickian behavior.

References

1. Pavlidou, S.; Papaspyrides, C. D. Prog Polym Sci 2008, 33, 1119.
2. Sengupta, R.; Chakraborty, S.; Bandyopadhyay, S.; Dasgupta, S.; Mukhopadhyay, R.; Auddy, K.; Deuri, A. S. Polym Eng Sci 2007, 47, 1956.
3. Thomas, S.; Stephen, R., Eds. Rubber Nanocomposites Preparation, Properties and Applications; John Wiley & Sons (Asia) Pte: Singapore, 2010.
4. Goettler, L. A.; Lee, K. Y.; Thakkar, H. Polym Rev 2007, 47, 291.
5. Kiliaris, P.; Papaspyrides, C. D. Prog Polym Sci 2010, 35, 7902.
6. Fu, S.; Feng, X.; Lauke, B.; Mai, Y. Compos Part B: Eng 2008, 39, 933.
7. Crosby, A. J.; Lee, J. Polym Rev 2007, 47, 217.
8. Chan, C.; Wu, J.; Li, J.; Cheung, Y. Polymer 2002, 43, 2981.
9. Yang, K.; Yang, Q.; Li, G.; Sun, Y.; Feng, D. Mater Lett 2006, 60, 805.
10. Yiping, H.; Guangmei, C.; Zhen, Y.; Hongwu, L.; Yong, W. Eur Polym J 2005, 41, 2753.
11. Jiang, G.; Huang, H. J Appl Polym Sci 2009, 114, 1687.
12. Gu, J.; Jia, D. S.; Cheng, R. S. Polym Plast Technol 2008, 47, 583.
13. Deshmane, C.; Yuan, Q.; Misra, R. D. K. Mater Sci Eng A 2007, 452, 592.
14. Wang, W.; Zeng, X.; Wang, G.; Chen, J. J Appl Polym Sci 2007, 106, 1932.
15. Chen, N.; Wan. C.; Zhang, Y.; Zhang, Y. Polym Test 2004, 23, 169.
16. Kemal, I.; Whittle, A.; Burford, R.; Vodenitcharova, T.; Hoffman, Polymer, 2009, 50, 4066.
17. Run, M.; Yao, C.; Wang, Y.; Song, H. Polym Compos 2008, 29, 1235.
18. Jain, R.; Narula, A. K.; Choudhary, V. J Appl Polym Sci 2009, 114, 2161.
19. Deng, C.; Chen, M.; Ao, N.; Yan. D.; Zheng, Z. J Appl Polym Sci 2006, 101, 3442.
20. Chakravarty, S. N.; Chakravarty, A. Elastomers and Plastics 2007, 39, 610.
21. Jin, F.; Park, S. Mater Sci Eng A 2008, 478, 406.
22. Mishra, S.; Sonawane, S. H.; Badgujar, N.; Gurav, K.; Patil, D. J Appl Polym Sci 2005, 96, 2563.
23. Mishra, S.; Shimpi, N. G.; Patil, U. D. J Polym Res 2007, 14, 449.
24. Mishra, S.; Shimpi, N. G. J Sci Ind res 2005, 64, 744.
25. Zhou, Y.; Wang, S.; Zhang, Y.; Zhang, Y. J Polym Sci Part B: Polym Phys 2006, 44, 1226.
26. Kader, M. A.; Kim, K.; Lee Y.-S.; Nah, C. J Mater Sci 2006, 41, 7341.
27. Das, A; Jurk, R; Stöckelhuber, K. W.; Heinrich, G. Macromol Mater Eng 2008, 293, 479.
28. Han, M.; Kim, H.; Kim, E. Nanotechnology 2006, 17, 403.
29. Wu, Y.; Jia, Q.; Yu, D.; Zhang, L. J Appl Polym Sci 2003, 89, 3855.
30. Sadhu, S.; Bhowmick, A. K. J Polym Sci Part B: Polym Phys 2004, 42, 1573.
31. Chung, J. W.; Han, S. J.; Kwak, S. Eur Polym J 2009, 45, 79.
32. Soares, B. G.; Oliveira, M.; Zaioncz, S.; Gomes, A. C. O.; Silva, A. A.; Santos, K. S.; Mauler, R. S. J Appl Polym Sci 2011, 119, 505.
33. Przepiórkowska, A.; Chrońska, K.; Prochon, M. J Appl Polym Sci 2009, 114, 800.
34. Yueyi, D.; Shijie, C.; Dapeng, W.; Shugao, Z. China Synth Rubber 2007, Available at: en.cnki.com.cn, CNKI:SUN: HCXF.0.2007-05-012.
35. Maged, S.; El-Nashar, D. E.; Maziad, N. A. Egypt J Sol 2003, 26, 241.
36. Nah, C.; Ryu, H. J.; Kim, W. D.; Chang, Y. W. Polym Int 2003, 52, 1359.
37. Mathew, G.; Rhee, J. M.; Lee, Y. S.; Park, D. H.; Nah, C. J Ind Eng Chem 2008, 14, 60.
38. Cai, H.; Li, S.; Tian, G.; Wang, H.; Wang, J. J Appl Polym Sci 2003, 87, 982.

39. Deng, C.; Chen, M.; Ao, N.; Yan, D.; Zheng, Z. J Appl Polym Sci 2006, 101, 3442.
40. Varghese, S.; Karger-Kocsis, J. J Appl Polym Sci 2004, 91, 813.
41. Manoj, K. C.; Kumari, P.; Rajesh, C.; Unnikrishnan, G. J Polym Res 2010, 17, 1.
42. Sujith, A.; Unnikrishnan, G. J Polym Res 2006, 13, 171.
43. Stephen, R.; Varghese, S.; Joseph, K.; Oommen, Z.; Thomas, S. J Membr Sci 2006, 282, 162.
44. Moly, K. A.; Bhagawan, S. S.; George, S. C.; Thomas, S. J Mater Sci 2007, 42, 4552.
45. Maiti, M.; Bhowmick, A. K. J Appl Polym Sci 2007, 105, 435.
46. Tang, C. Y.; Chen, D. Z.; Yue, T. M.; Chan, K. C.; Tsui, C. P.; Yu, P. H. F. Compos Sci Technol 2008, 68, 1927.
47. Sreekala, M. S.; Kumaran, M. S.; Thomas, S. Compos Part A Appl S 2002, 33, 763.
48. Crank, J. The Mathematics of Diffusion, 2nd ed.; Oxford University Press: Great Britain, 1975.